A 40-cM Region on Chromosome 14 Plays a Critical Role in the Development of Virus Persistence, Demyelination, Brain Pathology and Neurologic Deficits in a Murine Viral Model of Multiple Sclerosis

Shunya Nakane, Laurie J Zoecklein, Jeffrey D Gamez, Louisa M Papke, Kevin D Pavelko, Jean- François Bureau, Michel Brahic, Larry R Pease, Moses Rodriguez

RESEARCH ARTICLE

A 40-cM Region on Chromosome 14 Plays a Critical Role in the Development of Virus Persistence, Demyelination, Brain Pathology and Neurologic Deficits in a Murine Viral Model of Multiple Sclerosis

Shunya Nakane[1]; Laurie J. Zoecklein[1]; Jeffrey D. Gamez[1]; Louisa M. Papke[1]; Kevin D. Pavelko[1]; Jean-François Bureau[3]; Michel Brahic[3]; Larry R. Pease[2]; Moses Rodriguez[1, 2]

[1] Department of Neurology and [2]Immunology, Mayo Clinic and Foundation, Rochester, Minn.
[3] Unité des Virus Lents, URA CNRS 1930, Institut Pasteur, Paris, France.

Theiler's virus persists and induces immune-mediated demyelination in susceptible mice and serves as a model of multiple sclerosis. Previously, we identified 4 markers—*D14Mit54*, *D14Mit60*, *D14Mit61*, and *D14Mit90*—in a 40-cM region of chromosome 14 that are associated with demyelination in a cross between susceptible DBA/2 and resistant B10.D2 mice. We generated congenic-inbred mice to examine the contribution of this 40-cM region to disease. DBA Chr.14^{B10} mice, containing the chromosomal segment marked by the microsatellite polymorphisms, developed less spinal cord demyelination than did DBA/2 mice. More demyelination was found in the reciprocal congenic mouse B10.D2 Chr.14^{D2} than in the B10.D2 strain. Introduction of the DBA/2 chromosomal region onto the B10.D2 genetic background resulted in more severe disease in the striatum and cortex relative to B10.D2 mice. The importance of the marked region of chromosome 14 is indicated by the decrease in neurological performance using the Rotarod test during chronic disease in B10.D2 Chr.14^{D2} mice in comparison to B10.D2 mice. Viral replication was increased in B10.D2 Chr.14^{D2} mice as determined by quantitative real-time RT-PCR. These results indicate that the 40-cM region on chromosome 14 of DBA/2 mice contributes to viral persistence, subsequent demyelination, and loss of neurological function.

Brain Pathol 2003;13:519-533.

Introduction

Multiple sclerosis (MS) is the most common demyelinating disease of the central nervous system (CNS) in humans. MS is characterized by neurological deficits, including impaired vision, muscle weakness, sensory disturbance, and cerebellar ataxia (32, 47). Pathologic abnormalities include inflammatory demyelination, astrocyte scars known as plaques, and axonal injury or loss (10, 38). Genetic factors influence susceptibility, clinical course, and severity of the disease (24, 28, 60, 68).

There are 2 commonly accepted animal models of MS: *i)* Experimental autoimmune encephalomyelitis (EAE), a T-cell-mediated autoimmune disease of the CNS induced by immunization with myelin proteins or peptides (50), and *ii)* infection of mice with Theiler's murine encephalomyelitis virus (TMEV). TMEV establishes persistent infection in the CNS and leads to progressive demyelinating disease (19, 20, 52). The model provides a means to study both genetic and immunological factors in demyelination. Following intracerebral infection, TMEV induces chronic inflammatory demyelination and virus persistence in the spinal cord of susceptible strains of mice but is cleared from the CNS of resistant strains of mice (18, 55). The range of susceptibility or resistance to demyelination varies greatly among strains. SJL/J, DBA/2J, and PL/J mice are highly susceptible; C57BL/6J, C57BL/10J, and BALB/cJ are resistant; and C3H/J and AKR/J display intermediate susceptibility. Previous studies identified several loci associated with susceptibility or resistance to TMEV-induced demyelination, both major histocompatibility complex (MHC) and non-MHC linked (11, 13, 15, 45, 63). The effect of the H-2 region on susceptibility to demyelination was formally proven using H-2 congenic mice on a C57BL/10 background (54, 55). Mice with *f*, *p*, *q*, *r*, *s*, and *v* haplotypes were susceptible whereas mice with *b*, *d*, and *k* haplotypes were

Corresponding author:
Moses Rodriguez, Department of Neurology and Immunology, Mayo Clinic, 200 First St. S.W., Rochester, MN 55905, USA (E-mail: rodriguez.moses@mayo.edu)

resistant (54). Several groups have mapped a locus in the H-2D region of the MHC on chromosome 17 that plays a major role in resistance (15, 18, 55).

Although the H-2D gene has a major affect in controlling virus clearance or persistence caused by TMEV (4, 37, 59) other non H-2D genes for susceptibility have been mapped by linkage analysis. The genetic make-up of the strains analyzed determines the range of genes influencing susceptibility to TMEV induced demyelinating disease that can be investigated in each genetic cross. Among those identified are genes linked to the interferon (IFN)-γ locus on chromosome 10 and the myelin basic protein (MBP) locus on chromosome 18 (8, 9, 16). The *Tcrb* locus on chromosome 6 is also implicated, although deletion of Vβ genes characteristic of SJL/J mice and other strains is not responsible for susceptibility (44, 56, 58). More recently, Aubagnac et al reported a locus on chromosome 11, which affects susceptibility to clinical disease of *Ifngr*$^{-/-}$ mice and showed that inactivating the $\beta_2 m$ gene increases the viral load of SJL/J mice persistently infected by TMEV (2, 3).

Our analysis of a new set of genetic backgrounds involved intercrosses between DBA/2J mice, susceptible to TMEV-induced demyelination, and resistant B10.D2 mice. Both strains are *H-2*^{d}, the B10.D2 strain having been developed by breeding the H-2 region of the DBA/2J strain onto the C57BL/10 strain. Therefore, comparison of DBA/2J and B10.D2 strains identifies non H-2 loci involved in the susceptibility/resistance to demyelination. In a previous report, we identified 4 markers within a 40-cM region on chromosome 14 that were significantly associated with inflammation and demyelination (17) using linkage analysis in a (DBA/2J X B10.D2) F_2 intercross. To address definitively the contribution of chromosome 14 to TMEV-induced demyelination and virus persistence, we selected 7 microsatellite markers—*D14Mit207*, *D14Mit54*, *D14Mit61*, *D14Mit5*, *D14Mit90*, *D14Mit7*, and *D14Mit265*—to generate congenic strain of mice encompassing this 40-cM region. In the present study, we compared parameters of TMEV-induced demyelinating disease in susceptible DBA/2J, resistant B10.D2. We also investigated 2 new lines, DBA/2 Chr14^{B10} (DBA/2J congenic for the 40-cM region of chromosome 14 derived from B10.D2, and B10.D2 Chr14^{D2} (B10.D2 congenic for the 40-cM region of chromosome 14 derived from DBA/2J). We hypothesized that genes within the 40-cM region on chromosome 14 control virus persistence, development of demyelination, and the development of subsequent neurological deficits.

Materials and Methods

Virus. The Daniel's strain of TMEV (DA) was used for all in vivo experiments. The virus was grown in BHK-21cells and titrated by plaque assay in L2 cells as described previously (53). Purified virus was prepared from infected BHK-21 cells by ultracentrifugation on sucrose and cesium chloride gradient as described previously.

Mice. DBA/2J and B10.D2 mice were purchased from The Jackson Laboratory (Bar Harbor, Me), and bred in the animal facility of the Pasteur Institute. (DBA/2 × B10.D2) F1 mice were backcrossed nine times towards either the DBA/2 or the B10.D2 parental strain. At each generation during backcrossing, mice heterozygous for microsatellite markers *D14Mit207*, *D14Mit54*, *D14Mit61*, *D14Mit5*, *D14Mit90*, *D14Mit7* and *D14Mit265* were selected. The sequence and genomic position of the markers are available at *http://www.informatics.jax.org/*. Markers were separated by less than 8 cM to avoid double crossing over. After the ninth backcross, stabilization of the donor strain chromosome 14 interval on the recipient strain genetic background was obtained by crossing 2 heterozygous mice. The size of the interval that was introgressed (>42 cM) and the markers at the extremities were determined according to the confidence interval for linkage as given by the Mapmaker program. Mice were sent to Mayo Clinic for breeding. Handling of all animals conformed to the National Institutes of Health and Mayo Clinic institutional guidelines.

Preparation of spinal cords for pathologic analysis. On day 45 after TMEV infection, mice were anesthetized intraperitoneally with 10 mg of sodium pentobarbital and perfused by intracardiac puncture with Trump's fixative (phosphate-buffered 4% formaldehyde with 1.5% glutaraldehyde [pH 7.2]). Spinal cords were dissected and cut into one-mm blocks. Every third block was embedded in glycol methacrylate and stained with a modified erichrome stain with a cresyl violet counterstain to detect inflammation and demyelination (51). The rest of the spinal cord blocks were embedded in paraffin for immunoperoxidase staining for virus antigen. Detailed morphologic analysis was performed on 10 to 15 coronal spinal cord sections from each animal. A total of 1708 spinal cord quadrants were studied. Each quadrant from every third spinal cord block from each animal was scored for the presence of the particular pathologic abnormality. A maximum pathologic

score of 100 indicated that there was disease in every quadrant of every spinal cord block from a particular mouse. All analyses were done on coded samples without knowledge of the experimental groups.

Quantitation of pathologic findings in the brain. Brain pathology was assessed at days 7, 45, and 90 post-infection for each mouse strain. Following perfusion with Trump's fixative, 2 coronal cuts were made in the intact brain at time of removal from the skull (one section through the optic chiasm and a second section through the infundibulum). This allowed for systemic analysis of pathology of brainstem, cerebellum, cortex, hippocampus, corpus callosum, and striatum. Resulting slides were then stained with hematoxylin and eosin. Pathologic scores were assigned without knowledge of mouse strains to the following areas of brain: brainstem, cerebellum, cortex, hippocampus, corpus callosum, and striatum. Each area of brain was graded on a scale of 0 to 4 as follows: 0 = no pathology; 1 = no tissue destruction but only minimal inflammation; 2 = early tissue destruction (loss of architecture) and moderate inflammation; 3 = definite tissue destruction (demyelination, parenchymal damage, cell death, neurophagia, neuronal vacuolation); and 4 = necrosis (complete loss of all tissue elements with associated cellular debris). Meningeal inflammation was assessed and graded as follows: 0 = no inflammation; 1 = one cell layer of inflammation; 2 = two cell layers of inflammation; 3 = three cell layers of inflammation; and 4 = four or more cell layers of inflammation. Area with maximal extent of tissue damage was used for assessment of each brain region.

RNA isolation. The brain and spinal cords were removed from animals at 7, 21, 45, and 90 days after infection with TMEV. Total RNA was extracted from brain and spinal cord separately. Briefly, the tissues were frozen and stored in liquid nitrogen. Tissues samples were homogenized in RNA STAT-60 (one ml/100 mg tissue) (TEL-TEST, INC., Friendswood, Tx), and total RNA was isolated according to the manufacturer's recommendations. The RNA concentrations were determined by spectrophotometry. The RNA samples were adjusted to a concentration of 0.25 μg/μl and stored at -80ºC.

RT-PCR and real-time analysis. A fragment of the VP2 gene of TMEV, which codes for one of the capsid proteins, was amplified by RT-PCR. The sequences of the pair of primers were as follows: forward (5′-TGGTC GACTC TGTGG TTACG-3′) and reverse (5′-GCCGG TCTTG CAAAG ATAGT-3′). Gluceraldehyde-3-phosphate dehydrogenase (GAPDH) was used as a control for intersample variability. The sequences used for assaying the presence of GAPDH were: forward (5′-ACCAC CATGG AGAAG GC-3′) and reverse (5′-GGCAT GGACT GTGGT CATGA-3′). The sizes of PCR products amplified were: VP2 of DA virus, 238 base pairs (bp); GAPDH, 236 bp. Gene copy standards were generated for each set of samples. Standards were generated by serial 10-fold dilutions of plasmid cDNA. Standards were amplified in parallel with unknown samples by real-time quantitative RT-PCR using the LightCycler (Roche, Indianapolis, Ind). Analysis to generate standard curves was performed using LightCycler 3 software. Negative controls (omitting input cDNA) were also used in each PCR run to confirm the specificity of the PCR products. PCR products curves were linear across serial 10-fold dilutions, and the melting curve analysis indicated synthesis of a single homogenous product of the expected melting temperature. The reactions were done in 20-μl capillaries containing 7.0 mM Mg^{2+}, 10-pM concentrations of each forward and reverse primer, 4.0 μl of LightCycler-RT-PCR Reaction Mix SYBR Green I (LightCycler-RNA Amplification Kit SYBR Green I; Roche), 2 μl of resolution solution, 0.4 μl of LightCycler-RT-PCR Enzyme Mix, sterile H_2O, and 0.5 μg total RNA. Reaction conditions for RT-PCR for VP2 and GAPDH were as follows: reverse transcription at 55°C for 10 minutes, followed by denaturation at 95°C for 2 minutes, followed by 40 cycles of amplification. Amplification conditions were; denaturing at 95°C at 20°C/s without plateau phase, annealing at 57°C for 7 seconds, and extension 72°C for 15 seconds. The accumulation of products was monitored by SYBR Green fluorescence at the completion of each cycle. There was a direct relationship between the cycle number at which accumulation of PCR products became exponential and the log concentration of RNA molecules initially present in the RT-PCR reaction. The reaction conditions for melting curve analysis were as follows: denaturation to 95°C at 20°C/s without plateau phase, annealing at 60°C for 5 seconds, and denaturation to 95°C at 0.1°C/s, with continuous monitoring of SYBR Green fluorescence. RNA samples (n = 256) from DA virus infected DBA/2, DBA/2 Chr.14 B10.D2, B10.D2, and B10.D2 Chr14. DBA/2 mice were analyzed for GAPDH mRNA levels to determine the levels of mRNA per sample and the technical reproducibility. The amount of viral RNA was expressed as $\log_{10}$ virus

Strain	Number of mice	Meningeal inflammation	Demyelination	Number with demyelination	Meningeal inflammation*	Demyelination*
DBA/2	19	9.3 ± 2.2†	11.2 ± 2.4†	17	10.4 ± 2.3	12.5 ± 2.5†
DBA/2 Chr14^{B10}	19	3.0 ± 1.0‡	5.1 ± 1.5‡	9	4.2 ± 1.3	7.5 ± 1.9
B10.D2	20	0.16 ± 0.16§	0.16 ± 0.55§	1	1.9	1.9
B10.D2 Chr14^{D2}	72	1.1 ± 0.3	3.1 ± 0.6	32	2.0 ± 0.5	7.0 ± 1.9

Table 1. Spinal cord pathology in DBA and B10.D2 congenics.

* Meningeal Inflammation and Demyelination scores excluding animals that did not demyelinate.
† Significantly different than B10.D2 by Rank sum test ($p<0.05$)
‡ Significantly different than DBA/2 by Rank sum test ($p<0.05$)
§ Significantly different than B10.D2 Chr14D2 by Rank sum test ($p<0.05$)

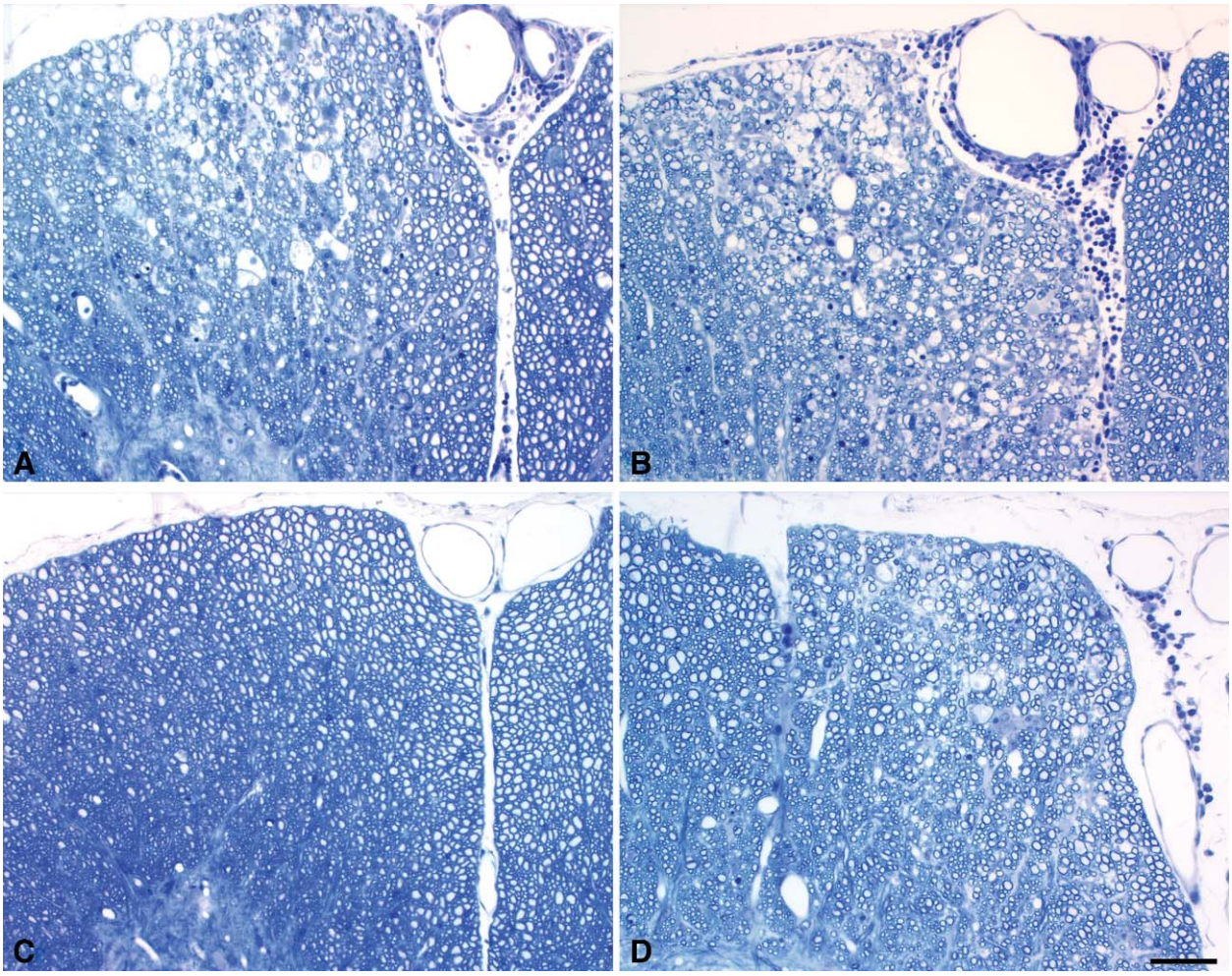

Figure 1. Examples of pathology in the spinal cord of (**A**) DBA/2, (**B**) DBA/2 Chr14^{B10}, (**C**) B10.D2, (**D**) B10.D2 Chr14^{D2} mice at day 45 after infection with TMEV. There was less demyelination in DBA/2 Chr14^{B10} as compared to DBA/2 (see Table 1). Note increased number of demyelinated axons in the spinal cord of B10.D2 Chr14^{D2} mice as compared with resistant B10.D2 mice. Spinal cords were embedded in glycol methacrylate and stained with a modified erichrome cresyl-violet stain. Sections such as these were used for quantitative analysis as shown in Table 1. Magnification for all pictures, ×20.

copy number per 0.5 μg RNA total. The GAPDH mRNA level per sample was 7.14 ± 0.015 (mean ± the SEM) (log_{10} virus copy number/0.5 μg RNA). Therefore, the marked variations in viral RNA levels in individual specimens could not be attributed to differences in amplifiable material. Eight mice were sacrificed at 7, 21, 45, and 90 days p.i., quantitative real-time RT-PCR was performed for the brains and spinal cords separately.

Immunohistochemical staining for DAV antigens. Immunocytochemistry was performed on paraffin-embedded brain and spinal cord sections, as previously described (52, 57). Slides were deparaffinized in xylene, and rehydrated through an ethanol series (absolute, 95 %, 70 %). The sections were immunostained with a polyclonal rabbit antiserum to purified TMEV strain DA virions by the avidin-biotin immunoperoxidase technique (Vector Laboratories, Burlingame, Calif). Slides were developed with a solution of 75 μg of Hanker-Yates reagent (p-phenylene diamine-procatechol [Polysciences, Inc., Warrington, Pa]). For quantitative analysis, a Zeiss microscope attached to a camera lucida was used to project the brain and spinal cord images onto a ZIDAS (Carl Zeiss Inc., Oberkochen, Germany) digitizing tablet. All samples were traced to determine area of brain stem, cortex, hippocampus, corpus callosum, striatum in brain, and spinal cord (calculated in square millimeters). Number of virus antigen (Ag) - positive cells for each mouse was counted and final data were expressed as number of viral-positive cells per area of brain and spinal cord. Five mice from each strain were sacrificed at 7, 21, 45, and 90 d.p.i.

Clinical assessment of disease using an accelerated rotarod assay. The Rotamex rotarod (Columbus Instruments, Columbus, Ohio) measures balance, coordination, and motor control and was used to assess neurological function in this study. The rotarod consists of a suspended rod powered by a variable speed motor capable of running at a fixed speed or accelerating a constant rate. Mice were trained and tested according to the protocol established by McGavern et al (41). Prior to injection with TMEV or sham: PBS (phosphate buffered saline) each mouse received 3 days of training using a constant speed protocol. This consisted of three 3-minute trials over 3 days (12 rpm on day 1, 13rpm on day 2, and 14 rpm on day 3). Mice were then tested using an accelerated assay (initial speed of 10 rpm accelerating at 10 rpm per minute until the mouse fell off). Rotarod performance was measured on days 21, 45, 90, and 180 following virus infection. All subsequent trials consisted of one day of constant speed training (three 3-minute trials at 14 rpm) and one day of accelerated speed testing (3 trials consisting of initial speed of 10 rpm and accelerating at 10 rpm per minute until the mouse fell off). The data was expressed as the speed in rpm (rotarod velocity) that occurred prior to the mouse falling at each time point.

Statistics. Pathology data of brain and spinal cord that were not normally distributed were evaluated by Rank sum test. We also divided brain pathology scores into *i)* mild (score of 0, 1, 2) and *ii)* severe (score of 3, 4), and evaluated statistical difference between the groups by Chi-square test. For Rotarod data, statistical differences between TMEV-infected and sham-infected data at each time point post-infection for each mouse strain was calculated using a student's *t* test. Virological data that were normally distributed was analyzed by one-way ANOVA. Pairwise comparisons were evaluated by Student-Newman-Keuls methods. For data that were not normally distributed, the one-way ANOVA of ranks was employed. The significance was set at $P<0.05$.

Results

A 40-cM segment of chromosome 14 plays a critical role in demyelination in spinal cord. We determined the contribution of genes within the 40-cM region of chromosome 14 in regulating demyelination in response to TMEV infection. We analyzed spinal cords obtained from DBA/2, DBA/2 $Chr14^{B10}$, B10.D2, and B10.D2 $Chr14^{D2}$ mice for the presence or absence of myelin destruction 45 days after viral infection (Table 1; Figure 1). Demyelination was detected in only one of 12 resistant B10.D2 mice. In contrast 32 of 72 B10.D2 $Chr14^{D2}$ mice showed demyelination ($P<0.05$). Therefore the presence of the chromosome 14 region of DBA/2 mice conferred susceptibility to the otherwise resistant B10.D2 genotype. In the reciprocal analysis, 17 of 19 susceptible DBA/2 mice, but only 9 of 19 mice DBA/2 Chr14B10 developed spinal cord demyelination ($P < 0.05$). These comparisons confirm the hypothesis that the DBA/2 and B10.D2 mouse lines differ with respect to genes on chromosome 14, governing the ability of TMEV to induce demyelinating disease.

We then assessed the severity of demyelinating disease in the 4 mouse lines by counting the number of spinal cord quadrants showing demyelination and inflammation in each strain. As indicated in Table 1, the extent of demyelination and meningeal inflammation in B10.D2 $Chr14^{D2}$ was significantly greater than in B10.D2 mice

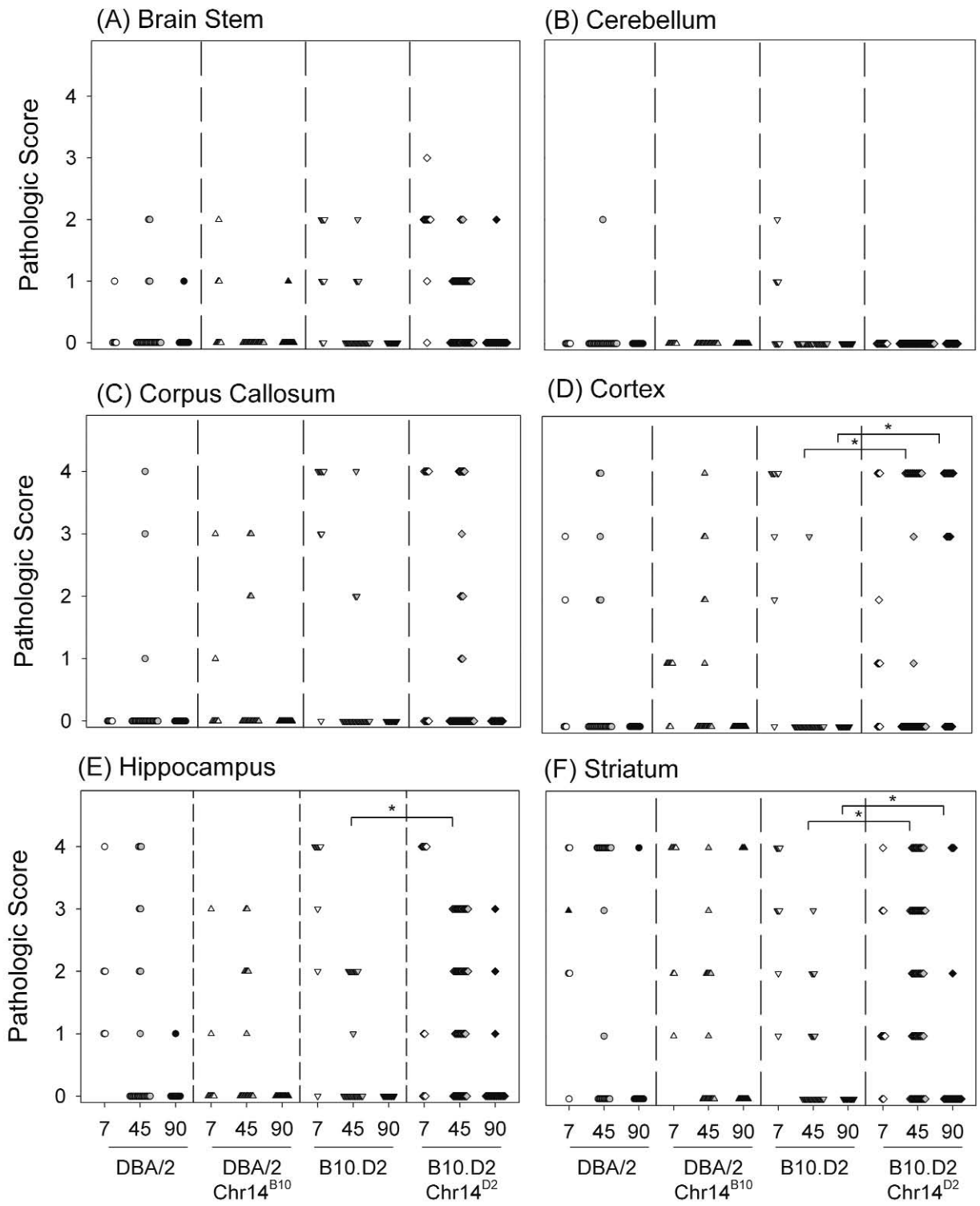
(A) Brain Stem
(B) Cerebellum
(C) Corpus Callosum
(D) Cortex
(E) Hippocampus
(F) Striatum
Pathologic Score
0
1
2
3
4
*
7 45 90
DBA/2
DBA/2 Chr14B10
B10.D2
B10.D2 Chr14D2

($P<0.05$). In contrast there were fewer quadrants with demyelinating lesions and meningeal inflammation in DBA/2 Chr14^{B10} mice as compared to wild-type DBA/2 mice (Table 1; demyelination, $P<0.05$; meningeal inflammation, $P<0.05$). In order to assess the possibility that these differences were due to a threshold affect governing the ability of virus to become established in spinal cord, we repeated the analysis by excluding all mice that did not show any signs of demyelination in the cord (Table 1). DBA/2 Chr14^{B10} mice continued to show less demyelination than DBA/2 mice ($P<0.05$, Rank order sum test). The extent of demyelination was very similar in B10.D2 Chr14^{D2} and DBA/2 Chr14^{B10} mice containing lesions. Too few lesions were present in resistant B10.D2 mice for inclusion in this comparison. The patterns of demyelination revealed by these comparisons are consistent with the hypothesis that genes within the 40-cM region of chromosome 14 influence the extent of demyelination in both strains. Genes from chromosome 14 of DBA/2 mice made normally resistant B10.D2 mice more susceptible to demyelination, whereas genes from chromosome 14 of B10.D2 lessened demyelination in DBA/2 mice.

Pathology in cortex and striatum is more severe in B10.D2. Chr14^{D2} than in B10.D2 mice. We next examined the brains of DBA/2, DBA/2 Chr14^{B10}, B10.D2 and B10.D2 Chr14^{D2} mice for signs of pathology (Figure 2). Similar levels of pathology were found at day 7, 45, and 90 p.i. in all areas of the brains of DBA/2 mice and DBA/2 Chr14^{B10} congenic mice. In contrast, significantly more pathology was observed at 45 and 90 days p.i. in the striatum ($P=0.0003$, $P=0.002$; Figure 2F) and in the hippocampus ($P=0.006$; Figure 2E) of B10.D2.Chr14^{D2} compared to B10.D2 mice. There was more brain pathology at 45 and 90 days p.i. in the cortex of B10.D2 Chr14^{D2} as compared to B10.D2 ($P=0.01$, $P=0.0007$; Figure 2D, respectively), indicating a contribution of genes from DBA/2 on chromosome 14 toward the determining the severity of inflammation and injury in the brain following virus infection. In addition, we found more severe inflammation and tissue destruction in the striatum, hippocampus and cortex of B10.D2 Chr14^{D2} as compared to the same region of brain in B10.D2 mice.

Chromosome 14 from DBA/2 is required for virus RNA persistence in the spinal cord. Because viral RNA persistence is a prerequisite for demyelination, we tested whether the mechanism for modulation of demyelination was secondary to a role of this 40-cM region in altering viral persistence. The amount of TMEV in the brain and spinal cord of infected mice was monitored by determining VP2 copy number using quantitative real-time RT-PCR. For these experiments, RNA was prepared separately from brain and spinal cord of DBA/2, DBA/2 Chr14^{B10}, B10.D2, and B10.D2 Chr14^{D2} mice at various time points after TMEV infection (Figure 3). In the brain (Figure 3A), the amount of viral RNA decreased in all strains as a function of time after infection. The decrease in B10.D2 mice was gradual. In DBA/2, DBA/2 Chr14^{B10}, and B10.D2 Chr14^{D2} mice, there was a stabilization of VP2 copy number between days 21 and 45, but all mice showed a decrease by 90 day post-infection. In the spinal cord (Figure 3B), there was a gradual decrease in VP2 specific RNA in the resistant B10.D2 mice as a function of time. In contrast, in susceptible DBA/2, and DBA/2 Chr14^{B10} mice, there was a stabilization of virus copy number from 7 to 45 d.p.i., but an increase of approximately 10 fold at 90d.p.i.. There was no statistical difference in the VP2 copy number between DBA/2 and DBA/2 Chr14^{B10} mice at any time point. In B10.D2 Chr14^{D2} mice, there was stabilization of virus copy number in the spinal cord from day 21 to 90 p.i.. There was 10 to 100 times more virus copy number in B10.D2 Chr14^{D2} mice as compared to B10.D2 mice at day 45 and 90 p.i. ($P=0.013$, $P<0.001$, respectively). The findings suggest an interaction between genes on chromosome 14 with genes elsewhere in the B10.D2 genome to curtail virus replication in the B10.D2 mouse. When either set of 2 genes was substituted by genes from the DBA/2 strain, virus replication increased.

We confirmed these findings in an analysis of virus protein expression by immunohistochemistry. Expression of TMEV antigens in the brains and spinal cords revealed the presence of virus in hippocampus and corpus callosum of DBA/2 mice at 7 and 21 days p.i (Figure 4). However, in late disease (45 to 90 days p.i.) viral antigen expression rapidly declined in brain, whereas it became predominant in spinal cord. Similarly, DBA/2 Chr14^{B10} mice had virus antigen positive cells in hip-

Figure 2. (Opposing page) Quantification of brain disease in DBA/2 (n = 41), DBA/2 Chr14^{B10} (n = 38), B10.D2 (n = 45), and B10.D2 Chr14^{D2} (n = 90) mice following TMEV infection. Each symbol represents an individual mouse graded at each area of the brain according to the scale detailed in the methods. B10.D2 Chr14^{D2} mice showed more severe disease in the cortex at 45 and 90 d.p.i. ($P=0.01$, $P=0.0007$; D), in the hippocampus at 45 d.p.i. ($P=0.006$; E), and in the striatum at 45 and 90d.p.i. ($P=0.0003$, $P=0.002$; F), when compared with the B10.D2 mice.

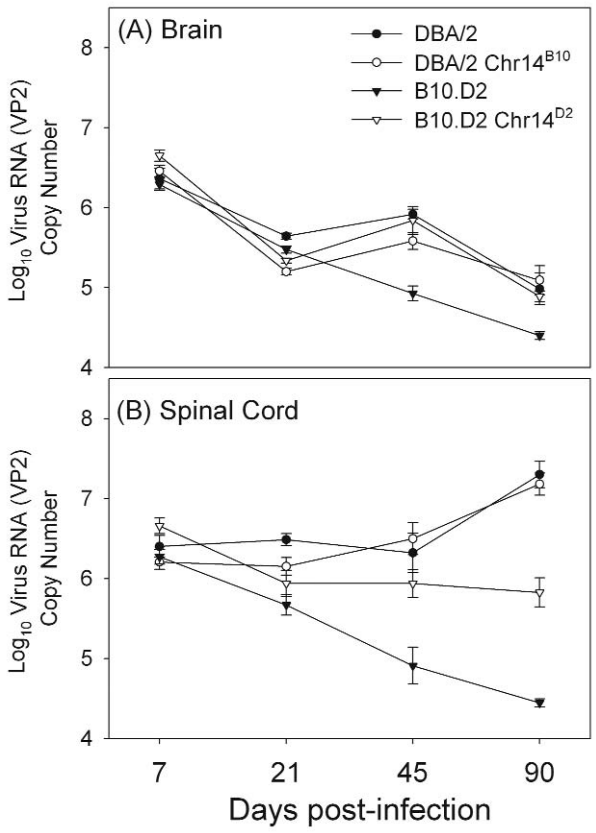

Figure 3. Levels of viral RNA in (**A**) brain and (**B**) spinal cord in DBA/2, DBA/2 Chr.14^{B10}, B10.D2, and B10.D2 Chr14^{D2} mice at 7, 21, 45, 90 days p.i.. Data are expressed as $\log_{10}$ virus copy number/0.5 μg total RNA. Mean and standard error values are shown for eight mice of each strain at each time point. VP2 RNA copy number in brain and spinal cord were analyzed separately for all strains to allow interstrain comparisons. Virus persistence correlated with presence of chromosome 14 of susceptible DBA/2 mice, since higher viral load was detected in CNS in B10.D2 Chr14^{D2} mice as compared to B10.D2 mice ($P = 0.032$; in the brain, $P<0.001$; in the spinal cord) (Pairwise comparisons were performed using the Student-Newman-Keuls method: $P<0.05$). In spinal cords from DBA/2 and DBA/2 Chr.14^{B10} mice, significant increases in VP2 viral RNA copy number were detected at 45, and 90 d.p.i. as compared to 7 and 21 d.p.i. ($P<0.001$). There was higher VP2 RNA copy number in the spinal cord as compared to the brain in both DBA/2 and DBA/2 Chr.14^{B10} at 45, and 90 d.p.i. ($P<0.001$). In B10.D2 mice only, there was no difference in viral load when comparing brain and spinal cord. However, in B10.D2 Chr14^{D2} mice, viral RNA copy number in the spinal cord was rather constant at all time points whereas viral RNA in brain decreased 21, 45, and 90 d.p.i.

pocampus and corpus callosum and in spinal cord at levels that were not statistically different from the levels seen in DBA/2 mice. Virus was rapidly cleared from most of brain and spinal cord of B10.D2 mice by 21 d.p.i..

Figure 4. (Opposing page) Immunostaining for virus antigen was performed using immunoperoxidase technique with polyclonal rabbit antibody to TMEV. A 10X objective was used to quantify DAV antigen positive cells. Area of brain and spinal cord was outlined manually and calculated with an image analysis system. Data are expressed as number of virus Ag positive cells per square millimeter. There was statistically significant more virus antigen positive cells in the brain stem of B10.D2 Chr14^{D2} mice as compared to B10.D2 mice at 7 days p.i. ($P = 0.010$). There was statistically significant more virus antigen positive cells in the spinal cord of B10.D2 Chr14^{D2} mice as compared to B10.D2 mice at 45 days p.i. ($P = 0.027$). Examples of immunoperoxidase staining in the spinal cord of (**G**) B10.D2, (**H**) B10.D2 Chr14^{D2} mice at day 45 after infection with TMEV. (×60).

The number of TMEV antigen-positive cells in brain stem of B10.D2 Chr14^{D2} mice was greater than that in B10.D2 mice ($P = 0.010$, Figure 4A). On day 45, more virus antigen positive cells were found in the spinal cord of B10.D2 Chr14^{D2} mice as well ($P = 0.027$, Figure 4F, H, G). Immunoperoxidase staining for TMEV in B10.D2 Chr14^{D2} mice was characterized by infection of cells resembling oligodendrocytes and macrophages, as demonstrated by the presence of TMEV antigen surrounding axons (Figure 4H). In contrast, minimal viral antigen expression was seen in the brain and spinal cord of B10.D2 mice (Figure 4G). These results demonstrate that the spinal cord is the primary site of TMEV antigen persistence in DBA/2 mice. This provides further support for the hypothesis that the ability of virus to persist during the chronic phase in the spinal cord is determined by interactions between non-MHC genes mapping to chromosome 14 and elsewhere in the B10.D2 genome.

The 40-cM segment of chromosome 14 from DBA/2 contributes to the severity of neurological deficits in the TMEV model of multiple sclerosis. We evaluated the role of the 40-cM region of chromosome 14 on severity of neurological deficits, using a rotarod assay to assess motor balance and coordination in sham (PBS)-infected and TMEV (DAV)-infected DBA/2, DBA/2 Chr14^{B10}, B10.D2, and B10.D2 Chr14^{D2} mice at 21, 45, 90, and 180 d.p.i.. To control for age and non-specific deficit due to injection, we compared all TMEV infected mice to sham infected animals at all time points. There was no statistical difference between infected and uninfected rotarod performances at day 0 p.i. (baseline) in all strains of mice. We found less time on the rotarod in TMEV-infected DBA/2 mice at 180 d.p.i. ($P = 0.025$, Figure 5A), and in TMEV-infected DBA/2 Chr14^{B10} mice at day 90 and 180 p.i. ($P = 0.006$, $P =$

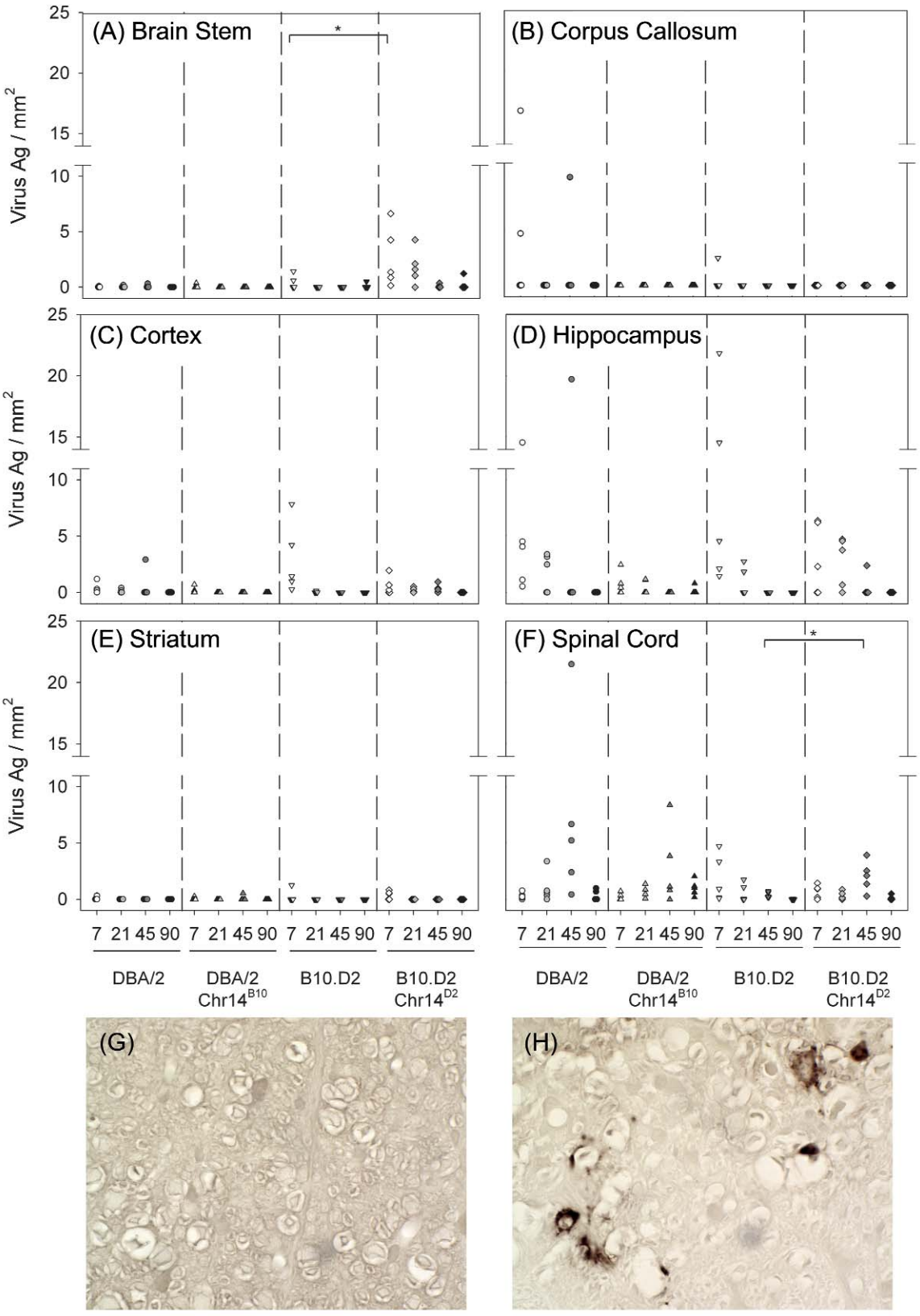
(A) Brain Stem
(B) Corpus Callosum
(C) Cortex
(D) Hippocampus
(E) Striatum
(F) Spinal Cord
Virus Ag / mm2
25
20
15
10
5
0
*
7 21 45 90 7 21 45 90 7 21 45 90 7 21 45 90
DBA/2
DBA/2 Chr14B10
B10.D2
B10.D2 Chr14D2
(G)
(H)

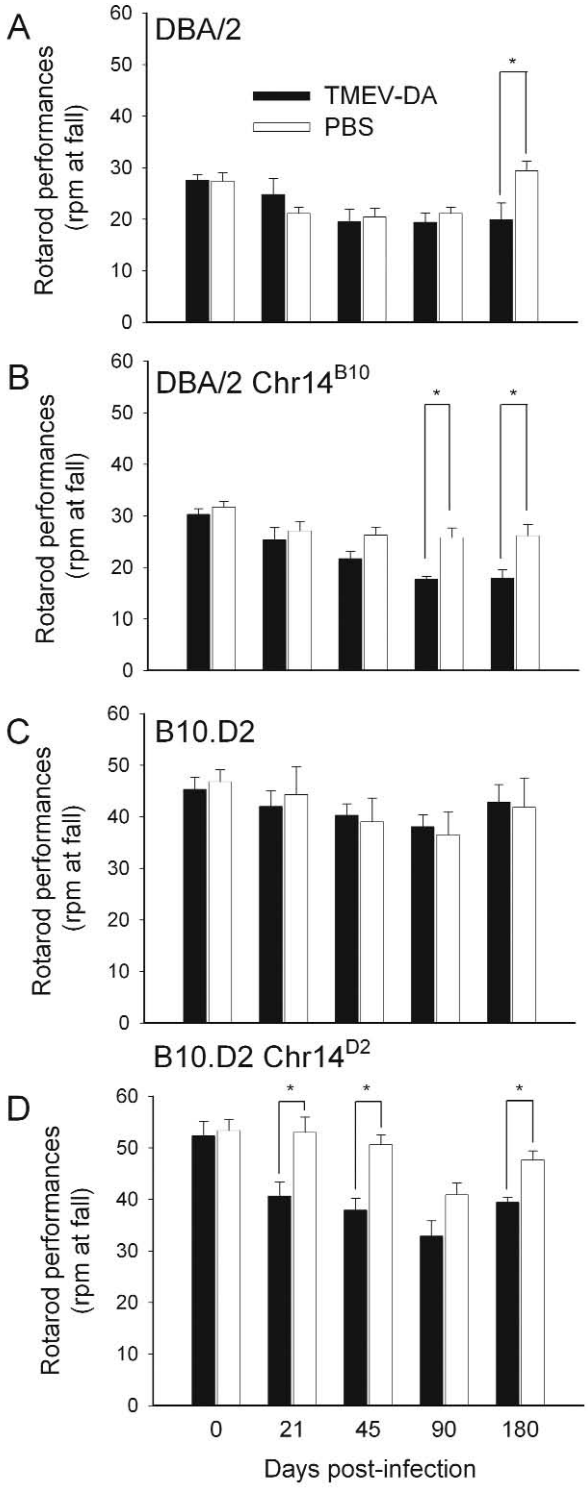

Figure 5. Assessment of motor coordination following TMEV infection using the rotarod assay. The rotarod velocity expressed as rpm (mean ± SEM) at the point the mice fell off the rotarod was determined in 6 to 11 mice for each experimental group. We compared rotarod velocity in infected versus sham-infected mice were analyzed to remove factors of age and injection from the analyses. TMEV-infected DBA/2 and DBA/2 Chr14^{B10} mice showed more deficits at the chronic phase as compared to uninfected mice of these strains. There was no statistical difference between rotarod performances in infected versus uninfected B10.D2 mice, while TMEV-infected B10.D2 Chr14^{D2} mice had statistically significant reductions in rotarod performance at 21, 45, and 180 d.p.i. compared to uninfected B10.D2 Chr14^{D2} mice ($P = 0.019$, $P = 0.004$, and $P = 0.004$, respectively). Asterisk denotes statistical significance.

0.014, respectively, Figure 5B), when compared to sham injected mice. In contrast, as we expected, no deficits were observed in infected versus uninfected B10.D2 mice (Figure 5C). However, TMEV-infected B10.D2 Chr14^{D2} mice had statistically significant reductions in rotarod performance at 21, 45, and 180 d.p.i. compared to uninfected B10.D2 Chr14^{D2} mice ($P = 0.019$, $P = 0.004$, and $P = 0.004$, respectively, Figure 5D). We conclude from these comparisons that genes present on chromosome 14 of susceptible DBA/2 mice are permissive to neurological injury in normally resistant B10.D2 strain of mice.

Discussion

We used crosses between susceptible DBA/2J mice and resistant B10.D2 mice to identify non H-2 genes involved in susceptibility or resistance to TMEV-induced demyelination (17). In our original manuscript, we identified 4 markers—*D14Mit54*, *D14Mit60*, *D14Mit61*, and *D14Mit90*—within a 40-cM region on chromosome 14 that were significantly associated with increased inflammation and more severe demyelination. Because 2 peaks were identified, one located close to *D14Mit54* and one near *D14Mit90*, it is possible that 2 distinct loci in this region are involved in determining susceptibility versus resistance to TMEV induced demyelinating disease. Previous experiments could not determine whether the genes on chromosome 14 exerted their effect directly on demyelination or by influencing viral persistence. In the present study, we generated congenic mice containing the region of chromosome 14 identified by the polymorphic DNA markers of B10.D2 in the context of the DBA/2 genome or the homologous region of chromosome 14 of DBA/2 in the context of the B10.D2 genome. Thus, we were able to test directly the role of the 40-cM region of chromosome 14 in viral RNA and antigen persistence and in promoting chronic demyelination under genetically controlled conditions.

We demonstrated that demyelination in the spinal cord was significantly less pronounced in DBA/2 Chr14^{B10} mice than in DBA/2 mice, whereas demyelination in the spinal cord in B10.D2 Chr14^{D2} mice was significantly greater than in B10.D2 mice. Using the rotarod assay we showed that B10.D2 Chr14^{D2} mice developed more severe neurological deficits than B10.D2 mice. These deficits could be attributed to events that occurred early, as progressive changes were observed after day 21 of infection.

We found that viral load in the spinal cord of B10.D2 Chr14^{D2} mice was higher than that observed in resistant B10.D2 mice. This is consistent with the hypothesis that the 40-cM region of chromosome 14 of DBA/2 mice contains genes controlling virus persistence and subsequently TMEV-induced demyelination.

However, not all the data fits with the simple hypothesis that this region alone distinguished susceptibility to virus in these 2 strains. The fact that viral load in the spinal cord of DBA/2 mice was similar to that in DBA/2 Chr14^{B10} mice indicates that other genes present in the B10.D2 mouse may interact with the genes on chromosome 14 to confer resistance to virus.

Another indication of the importance of genes on chromosome 14 was the finding that the percentage of mice showing demyelination was smaller in DBA/2 Chr14B10 than in DBA/2 mice. Of interest was the finding that DBA/2 Chr14^{B10} mice showed a 2-fold decrease in extent of demyelination compared to DBA/2 mice even though the levels of viral RNA and viral antigen in the spinal cord were not different. These data support the view that the 40-cM region of chromosome 14 in B10.D2 can modulate the severity of demyelination independent of the levels of persisting virus.

We propose the following model to explain susceptibility versus resistance to virus-induced demyelination following TMEV infection. Virus persistence is an absolute requirement for demyelination to develop. The major determinant of susceptibility is the class I MHC D region as demonstrated in earlier studies using MHC recombinant and transgenic mice (4, 18, 54, 55). If the appropriate class I MHC alleles are present, a rapid and vigorous CTL response against the virus develops within 7 days of

cM	Marker	*Symbol*	Name
5.5	**D14Mit 207**		
6.0		*Dnahc 3*	Dynein, axon, heavy chain 3
8.0		*Cacna1d*	Calcium channel, voltage-dependent, L type, alpha
		Dnahc 1	Dynein, axon, heavy chain 1
12.0		*Idd12*	Insulin dependent diabetes susceptibility - 12
12.5	**D14Mit54**		
13.0		*Bmpr*	Bone morphogenic receptor for Bmp2 and Bmp4
14.0		*Bmp4*	bone morphogenetic protein 4
17.0	**D14Mit61**		
19.5		*Gja3*	gap junction membrane channel protein alpha-3
		Gja2	gap junction membrane channel protein beta-2
		Tcra	T cell receptor alpha chain
		Tcrd	T cell receptor delta chain
19.7		*Tcra-C*	T cell receptor alpha, constant region
		Tcra-J	T cell receptor alpha, joining region
		Tcra-V	T cell receptor alpha, variable region
		Tcrd-C	T cell receptor delta, constant region
		Tcrd-D	T cell receptor delta, D region
		Tcrd-J	T cell receptor delta, joining region
		Tcrd-V	T cell receptor delta, variable region
20.0		*Bcl2l2*	Bcl2-like2
20.5		*Ctsg*	cathepsin G
		Gzmb-g	granzyme B-G
21.5		*Isgf3g*	interferon dependent positive acting transcription factor
22.5	**D14Mit5**		
28.5		*Ctsb*	cathepsin B
		Nfl	neurofilament, light polypeptide
		Nfm	neurofilament, medium polypeptide
30.5		*amd*	autoimmune myocardial disease
36.5		*Dad1*	defender against cell death 1
	D14Mit90		
44.5	**D14Mit7**		
47.0		*Ccnb1-rs12*	cyclin B1, related sequence 12
48.0	**D14Mit265**		

Table 2. 40-cM region of chromosome 14.

infection. We identified $VP2_{121-130}$ as the immunodominant viral epitope in H-$2D^b$ mice (22, 34, 35). The critical class I-restricted viral epitope is unknown in H-$2D^d$ mice. We suspect that B10.D2 mice clear the virus by mounting a strong CTL response, whereas in DBA/2 mice the response is weak and delayed thus predisposing to viral persistence. The present studies however indicate that development of virus persistence may also depend on other non-MHC genes that abrogate the protective CTL response in H-$2D^{b,\ d,\ or\ k}$ mice. Genes in the DBA/2 mouse, mapping into the 40-cM region of chromosome 14, undermine the protective responses found in B10.D2 mice, resulting in virus persistence and subsequent demyelination in B10.D2 $Chr14^{D2}$ mice despite the presence of a protective MHC genotype. Other genes that may function to influence virus persistence include a gene on chromosome 10 linked to IFN-γ and a gene on chromosome 18 linked to MBP (8, 9, 16). Once virus persistence is established, other genes appear to control severity of demyelination. The present experiments indicate that one of the genes that modulate severity of demyelination may be on the 40-cM region on chromosome 14 of B10.D2. This gene down-regulates the extent of demyelination, as DBA/2 $Chr14^{B10}$ mice develop less demyelination than DBA/2 mice, despite equivalent levels of virus RNA persistence in both strains.

Other genes likely control how severe neurological deficits are once demyelination is established. A locus of chromosome 11 that affects severity of clinical disease in IFN-γ receptor -/- mice may be such a gene (2). The severity of neurological deficit correlates best with axonal loss (42) or axonal dysfunction (65) rather than with the extent of demyelination.

There are approximately 100 known genes in the 40-cM region on chromosome 14 (1). Any of 14 genes which include dynein axon heavy chain, L-type voltage-dependent calcium channel (36), gap junction membrane protein, neurofilament, insulin dependent diabetes susceptibility, bone morphogenetic protein, T-cell receptor alpha and delta chain, Bcl-w, cathepsin B and G, granzyme, interferon stimulated gene factor 3, autoimmune myocardial disease, defender against apoptotic death 1, and cyclin B1, may be candidates for the control of pathologic abnormalities and viral persistence. Genes such as dyneins that are multisubunit mechanochemical enzymes capable of interacting with microtubles to generate force (67) could contribute to axonal injury. Anti-light neurofilament subunit antibody may serve as a marker for axonal loss and disease progression in MS (61, 62). Members of bone morphogenetic protein (BMP) family are implicated in multiple aspects in cerebral cortex development (26, 40) and in oligodendrocyte lineage commitment (26, 39, 40, 43).

A number of genes identified within this 40-cM segment may interact with the immune system to influence TMEV demyelination and neurologic deficits and may play a role in MS. These include T-cell receptor genes (5, 23, 27, 31), Bcl-2, Bcl-w gene, Bax and Bak (25), defender against apoptotic death (Dad) 1 (33), interferon stimulated gene factor (12), cathepsin (6,7) and perforin (69, 70). MS and other autoimmune diseases such as rheumatoid arthritis, and psoriasis is thought to be mediated by autoreactive T-cells (21, 66). T-cell infiltrates are mainly composed of TCR-$\alpha\beta^+CD4^+$ and TCR-$\alpha\beta^+CD4^+$ as well as TCR-γ/δ^+ T-cells. Several studies have analyzed TCR-α/β repertoire expressed in the lesions (5, 14). Hafler et al (27) created a database to analyze these sequences related to the human and experimental demyelinating disease, MS and EAE, respectively. In EAE, T-cells specific for MBP preferentially utilize Vα2 and Vβ8.2 genes in their TCR (29). Oksenberg et al (49) used PCR to amplify TCR Vα sequences from transcripts derived from MS brain lesions. The results showed that TCR Vα gene expression in MS brain lesion is restricted. Offner et al (48) analyzed TCR V genes, and they found TCR Vα8 and Vβ5 were utilized more frequently in MS patients than non-MS patients in response to MBP. We previously reported that TCR beta-complex did not influence susceptibility to Theiler's virus-induced demyelinating disease (21). We will focus on TCR α gene within 40-cM region on chromosome 14 in the future. Cathepsin G is tightly linked to the CTLA-1 locus on murine chromosome 14 (30). B7-CD28 costimulation is necessary for the activation of lytic function, ie, granzyme B or CTLA-1 in cytotoxic T-cell precursors. Perforin/granzyme-induced apoptosis is a major pathway used by cytotoxic lymphocytes to eliminate virus-infected cells (64). The mechanism by which oligodendrocytes are removed in demyelinating diseases may involve perforin (69, 70). We previously demonstrated that perforin-mediated cytotoxic effector function is necessary for viral clearance, and may directly contribute to development of neurologic deficits and axonal injury after demyelination in the TMEV model (46).

Determining the precise genes within the 40-cM region on chromosome 14 that influence TMEV disease will be a major focus of our research in the future. The congenic-inbred mice reported in this manuscript are a valuable resource to map the appropriate gene.

Because insertions of these genes were sufficient to influence disease, it is likely that the gene in isolation will be critical in understanding both virus persistence and demyelination. It is possible that a similar syntenic area in the human genome may prove to influence a disease such as MS.

Acknowledgments

This work was supported by grants from National Institute of Health (NS24180, NS34129, and PO1-NS38468). Work done at the Institut Pasteur was supported by Institut Pasteur, CNRS and the National Multiple Sclerosis Society. We would like to thank Mable Pierce for the processing of plastic-embedded section from the spinal cord.

References

1. Abbadi N, Nadeau JH (1998) Encyclopedia of the mouse genome VII. Mouse chromosome 14. *Mamm Genome* 8:S275-291.
2. Aubagnac S, Brahic M, Bureau JF (1999) Viral load and a locus on chromosome 11 affect the late clinical disease caused by Theiler's virus. *J Virol* 73:7965-7791.
3. Aubagnac S, Brahic M, Bureau JF (2001) Viral load increases in SJL/J mice persistently infected by Theiler's virus after inactivation of the β_2m gene. *J Virol* 75:7723-7726.
4. Azoulay-Cayla A, Syan S, Brahic M, Bureau JF (2001) Roles of the *H-2D*^{b} and *H-K*^{b} genes in resistance to persistent Theiler's murine encephalomyelitis virus infection of the central nervous system. *J Gen Virol* 82:1043-1047.
5. Battistini L, Selmaj K, Kowal C, Ohmen J, Modlin RL, Raine CS, Brosnan CF (1995) Multiple sclerosis: limited diversity of the Vδ 2-Jδ 3 T-cell receptor in chronic active lesions. *Ann Neurol* 37:198-203.
6. Bever CT Jr, Panitch HS, Johnson KP (1994) Increased cathepsin B activity in peripheral blood mononuclear cells of multiple sclerosis patients. *Neurology* 44:745-748.
7. Bever CT Jr, Garver DW (1995) Increased cathepsin B activity in multiple sclerosis brain. *J Neurol Sci* 131:71-73.
8. Bihl F, Pena-Rossi C, Guenet JL, Brahic M, Bureau JF (1997) The shiverer mutation affects the persistence of Theiler's virus in the central nervous system. *J Virol* 71:5025-5030.
9. Bihl F, Brahic M, Bureau JF (1999) Two loci, *Tmevp2* and *Tmevp3*, located on the telomeric region of chromosome 10, control the persistence of Theiler's virus in the central nervous system of mice. *Genetics* 52:385-392.
10. Bjartmar C, Trapp BD (2001) Axonal and neuronal degeneration in multiple sclerosis: mechanisms and functional consequences. *Curr Opin Neurol* 14:271-278.
11. Blankenhorn EP, Stranford SA (1992) Genetic factors in demyelinating diseases: genes that control demyelination due to experimental allergic encephalomyelitis (EAE) and Theiler's murine encephalitis virus. *Reg Immunol* 4:331-343.
12. Bluyssen AR, Durbin JE, Levy DE (1996) ISGF3γ p48, a specificity switch for interferon activated transcription factors. *Cytokine Growth Factor Rev* 7:11-17.
13. Brahic M, Bureau JF (1998) Genetics of susceptibility to Theiler's virus infection. *Bioessays* 20:627-633.
14. Brosnan CF, Raine CS (1996) Mechanisms of immune injury in multiple sclerosis. *Brain Pathol* 6:243-257.
15. Bureau JF, Montagutelli X, Lefebvre S, Guenet JL, Pla M, Brahic M (1992) The interaction of two groups of murine genes determines the persistence of Theiler's virus in the central nervous system. *J Virol* 66:4698-4704.
16. Bureau JF, Montagutelli X, Bihl F, Lefebvre S, Guenet JL, Brahic M (1993) Mapping loci influencing the persistence of Theiler's virus in the murine central nervous system. *Nat Genet* 5:87-91.
17. Bureau JF, Drescher KM, Pease LR, Vikoren T, Delcroix M, Zoecklein L, Brahic M, Rodriguez M (1998) Chromosome 14 contains determinants that regulate susceptibility to Theiler's virus-induced demyelination in the mouse. *Genetics* 148:1941-1949.
18. Clatch RJ, Melvold RW, Miller SD, Lipton HL (1985) Theiler's murine encephalomyelitis virus (TMEV)-induced demyelinating disease in mice is influenced by the H-2D region: correlation with TEMV-specific delayed-type hypersensitivity. *J Immunol* 135:1408-1414.
19. Dal Canto MC, Lipton HL (1977) Multiple sclerosis. Animal model: Theiler's virus infection in mice. *Am J Pathol* 88:497-500.
20. Dal Canto MC, Lipton HL (1977) A new model of persistent viral infection with primary demyelination. *Neurol Neurocir Psiquiatr* 18(2-3 Suppl):455-467.
21. DerSimonian H, Sugita M, Glass DN, Maier AL, Weinblatt ME, Reme T, Brenner MB (1993) Clonal V _12.1+ T-cell expansions in the peripheral blood of rheumatoid arthritis patients. *J Exp Med* 177:1623-1631.
22. Dethlefs S, Escriou N, Brahic M, van der Werf S, Larsson-Sciard EL (1997) Theiler's virus and Mengo virus induce cross-reactive cytotoxic T lymphocytes restricted to the same immunodominant VP2 epitope in C57BL/6 mice. *J Virol* 71:5361-5365.
23. Drescher KM, Johnston SL, Hogancamp W, Nabozny GH, David CS, Rimm IJ, Wettstein PJ, Rodriguez M (2000) $V_\beta 8^+$ T-cells protect from demyelinating disease in a viral model of multiple sclerosis. *Int Immunol* 12:271-280.
24. Ebers GC, Kukay K, Bulman DE, Sadovnick AD, Rice G, Anderson C, Armstrong H, Cousin K, Bell RB, Hader W, Paty DW, Hashimoto S, Oger J, Duquette P, Warren S, Gray T, O'Connor P, Nath A, Auty A, Metz L, Francis G, Paulseth JE, Murray TJ, Pryse-Phillips W, Nelson R, Freedman M, Brunet D, Bouchard JP, Hinds D, Risch N (1996) A full genome search in multiple sclerosis. *Nat Genet* 13:472-476.

25. Gibson L, Holmgreen SP, Huang DC, Bernard O, Copeland NG, Jenkins NA, Sutherland GR, Baker E, Adams JM, Cory S (1996) bcl-w, a novel member of the bcl-2 family, promotes cell survival. *Oncogene* 13:665-675.

26. Gross RE, Mehler MF, Mabie PC, Zang Z, Santschi L, Kessler JA (1996) Bone morphogenetic proteins promote astroglial lineage commitment by mammalian subventricular zone progenitor cells. *Neuron* 17:595-606.

27. Hafler DA, Saadeh MG, Kuchroo VK, Milford E, Steinman L (1996) TCR usage in human and experimental demyelinating disease. *Immunol Today* 17:152-159.

28. Haines JL, Ter-Minassian M, Bazyk A, Gusella JF, Kim DJ, Terwedow H, Pericak-Vance MA, Rimmler JB, Haynes CS, Roses AD, Lee A, Shaner B, Menold M, Seboun E, Fitoussi RP, Gartioux C, Reyes C, Ribierre F, Gyapay G, Weissenbach J, Hauser SL, Goodkin DE, Lincoln R, Usuku K, Garcia-Merino A, Gatto N, Young S, Oksenberg JR (1996) A complete genomic screen for multiple sclerosis underscores a role for the major histocompatability complex. The Multiple Sclerosis Genetics Group. *Nat Genet* 13:469-471.

29. Heber-Katz E, Acha-Orbea H (1989) The V-region disease hypothesis: evidence from autoimmune encephalomyelitis. *Immunol Today* 10:164-169.

30. Heusel JW, Scarpati EM, Jenkins NA, Gilbert DJ, Copeland NG, Shapiro SD, Ley TJ (1993) Molecular cloning, chromosomal location, and tissue-specific expression of the murine cathepsin G gene. *Blood* 81:1614-1623.

31. Hillert J, Leng C, Olerup O (1992) T-cell receptor α chain germline gene polymorphisms in multiple sclerosis. *Neurology* 42:80-84.

32. Hohlfeld R (1997) Biotechnical agents for the immunotherapy of multiple sclerosis: principles, problems and perspectives. *Brain* 120:865-916.

33. Hong NA, Kabra NH, Hsieh SN, Cado D, Winoto A (1999) In vivo overexpression of Dad1, the defender against apoptotic death-1, enhances T-cell proliferation but does not protect against apoptosis. *J Immunol* 163:1888-1893.

34. Johnson AJ, Njenga MK, Hansen MJ, Kuhns ST, Chen L, Rodriguez M, Pease LR (1999) Prevalent class I-restricted T-cell response to the Theiler's virus epitope D^b: $VP2_{121-130}$ in the absence of endogenous CD4 help, tumor necrosis factor alpha, gamma interferon, perforin, or costimulation through CD28. *J Virol* 73:3702-3708.

35. Johnson AJ, Upshaw J, Pavelko KD, Rodriguez M, Pease LR (2001) Preservation of motor function by inhibition of CD8+ virus peptide-specific T-cells in Theiler's virus infection. *FASEB J* 15:2760-2762.

36. Kornek B, Storch MK, Bauer J, Djamshidian A, Weissert R, Wallstroem E, Stefferl A, Zimprich F, Olsson T, Linington C, Schmidbauer M, Lassmann H (2001) Distribution of a calcium channel subunit in dystrophic axons in multiple sclerosis and experimental autoimmune encephalomyelitis. *Brain* 124:1114-1124.

37. Lipton HL, Melvold R, Miller SD, Dal Canto MC (1995) Mutation of a major histocompatibility class I locus, H-2D, leads to an increased virus burden and disease susceptibility in Theiler's virus-induced demyelinating disease. *J Neurovirol* 1:138-144.

38. Lucchinetti C, Bruck W, Noseworthy J (2001) Multiple sclerosis: recent developments in neuropathology, pathogenesis, magnetic resonance imaging studies and treatment. *Curr Opin Neurol* 14:259-269.

39. Mabie PC, Mehler MF, Marmur R, Papavasiliou A, Song Q, Kessler JA (1997) Bone morphogenetic proteins induce astroglial differentiation of oligodendroglial-astroglial progenitor cells. *J Neurosci* 17:4112-4120.

40. Mabie PC, Mehler MF, Kessler JA (1999) Multiple roles of bone morphogenetic protein signaling in the regulation of cortical cell number and phenotype. *J Neurosci* 19:7077-7088.

41. McGavern DB, Zoecklein L, Drescher KM, Rodriguez M (1999) Quantitative assessment of neurologic deficits in a chronic progressive murine model of CNS demyelination. *Exp Neurol* 158:171-181.

42. McGavern DB, Murray PD, Rivera-Quinones C, Schmelzer JD, Low PA, Rodriguez M (2000) Axonal loss results in spinal cord atrophy, electrophysiological abnormalities and neurological deficits following demyelination in a chronic inflammatory model of multiple sclerosis. *Brain* 123:519-531.

43. Mehler MF, Mabie PC, Zhu G, Gokhan S, Kessler JA (2000) Developmental changes in progenitor cell responsiveness to bone morphogenetic proteins differentially modulate progressive CNS lineage fate. *Dev Neurosci* 22:74-85.

44. Melvold RW, Jokinen DM, Knobler RL, Lipton HL (1987) Variations in genetic control of susceptibility to Theiler's murine encephalomyelitis virus (TMEV)-induced demyelinating disease. I. Differences between susceptible SJL/J and resistant BALB/c strains map near the T-cell β-chain constant gene on chromosome 6. *J Immunol* 138:1429-1433.

45. Monteyne P, Bureau JF, Brahic M (1997) The infection of mouse by Theiler's virus: from genetics to immunology. *Immunol Rev* 159:163-176.

46. Murray PD, McGavern DB, Lin X, Njenga MK, Leibowitz J, Pease LR, Rodriguez M (1998) Perforin-dependent neurologic injury in a viral model of multiple sclerosis. *J Neurosci* 18:7306-7314.

47. Noseworthy JH, Lucchinetti C, Rodriguez M, Weinshenker BG (2000) Multiple sclerosis. *N Engl J Med* 243:938-950.

48. Offner H, Vandenbark AA (1999) T-cell receptor V genes in multiple sclerosis: increased use of TCRAV8 and TCRBV5 in MBP-specific clones. *Int Rev Immunol* 18:9-36.

49. Oksenberg JR, Stuart S, Begovich AB, Bell RB, Erlich HA, Steinman L, Bernard CC (1990) Limited heterogeneity of rearranged T-cell receptor V αtranscripts in brains of multiple sclerosis patients. *Nature* 24:344-346.

50. Owens T, Sriram S (1995) The immunology of multiple sclerosis and its animal model, experimental allergic encephalomyelitis. *Neurol Clin* 1995; 13:51-73.

51. Pierce M, Rodriguez M (1989) Erichrome stain for myelin on osmicated tissue embedded in glycol methacrylate plastic. *J Histotechnol* 12:35-36.

52. Rodriguez M, Leibowitz JL, Lampert PW (1983) Persistent infection of oligodendrocytes in Theiler's virus-induced encephalomyelitis. *Ann Neurol* 13:426-433.

53. Rodriguez M, Leibowitz JL, Powell HC, Lampert PW (1983) Neonatal infection with the Daniels strain of Theiler's murine encephalomyelitis virus. *Lab Invest* 49:672-679.

54. Rodriguez M, David CS (1985) Demyelination induced by Theiler's virus: influence of the H-2 haplotype. *J Immunol* 135:2145-2148.

55. Rodriguez M, Leibowitz J, David CS (1986) Susceptibility to Theiler's virus-induced demyelination. Mapping of the gene within the H-2D region. *J Exp Med* 163:620-631.

56. Rodriguez M, Patick AK, Pease LR, David CS (1992) Role of T-cell receptor Vβ genes in Theiler's virus-induced demyelination of mice. *J Immunol* 148:921-927.

57. Rodriguez M, Dunkel AJ, Thiemann RL, Leibowitz J, Zijlstra M, Jaenisch R (1993) Abrogation of resistance to Theiler's virus-induced demyelination in H-2^b mice deficient in β2-microglobulin. *J Immunol* 151:266-276.

58. Rodriguez M, Nabozny GH, Thiemann RL, David CS (1994) Influence of deletion of T-cell receptor V_β genes on the Theiler's virus model of multiple sclerosis. *Autoimmunity* 19:221-230.

59. Rodriguez M, David CS (1995) H-2 D^d transgene suppresses Theiler's virus-induced demyelination in susceptible strains of mice. *J Neurovirol* 1:111-117.

60. Sawcer S, Jones HB, Feakes R, Gray J, Smaldon N, Chataway J, Robertson N, Clayton D, Goodfellow PN, Compston A (1996) A genome screen in multiple sclerosis reveals susceptibility loci on chromosome 6p21 and 17q22. *Nat Genet* 13:464-468.

61. Semra YK, Seidi OA, Sharief MK. (2002) Heightened intrathecal release of axonal cytoskeletal proteins in multiple sclerosis is associated with progressive disease and clinical disability. *J Neuroimmunol* 122:132-139.

62. Silber E, Semra YK, Gregson NA, Sharief MK (2002) Patients with progressive multiple sclerosis have elevated antibodies to neurofilament subunit. *Neurology* 58:1372-1381.

63. Teuscher C, Rhein DM, Livingstone KD, Paynter RA, Doerge RW, Nicholson SM, Melvold RW (1997) Evidence that *Tmevd2* and *eae3* may represent either a common locus or members of a gene complex controlling susceptibility to immunologically mediated demyelination in mice. *J Immunol* 159:4930-4934.

64. Trapani JA, Smyth MJ (2002) Functional significance of the perforin/granzyme cell death pathway. *Nat Rev Immunol* 2:735-747.

65. Ure DR, Rodriguez M (2002) Preservation of neurologic function during inflammatory demyelination correlates with axon sparing in a mouse model of multiple sclerosis. *Neuroscience* 111:399-411.

66. Vandenbark AA, Morgan E, Bartholomew R, Bourdette D, Whitham R, Carlo D, Gold D, Hashim G, Offner H (2001) TCR peptide therapy in human autoimmune diseases. *Neurochem Res* 26:713-730.

67. Vaughan KT, Mikami A, Paschal BM, Holzbaur EL, Hughes SM, Echeverri CJ, Moore KJ, Gilbert DJ, Copeland NG, Jenkins NA, Vallee RB (1996) Multiple mouse chromosomal loci for dynein-based motility. *Genomics* 36:29-38.

68. Weinshenker BG, Santrach P, Bissonet AS, McDonnell SK, Schaid D, Moore SB, Rodriguez M (1998) Major histocompatibility complex class II alleles and the course and outcome of MS: a population-based study. *Neurology* 51:742-747.

69. Zeine R, Pon R, Ladiwala U, Antel JP, Filion LG, Freedman MS (1998) Mechanism of γδ T-cell-induced human oligodendrocyte cytotoxicity: relevance to multiple sclerosis. *J Neuroimmunol* 87:49-61.

70. Zeine R, Cammer W, Barbarese E, Liu CC, Raine CS (2001) Structural dynamics of oligodendrocyte lysis by perforin in culture: relevance to multiple sclerosis. *J Neurosci Res* 64:380-391.